

Long Range Probabilistic Forecasting in Time-Series using High Order Statistics

Prathamesh Deshpande and Sunita Sarawagi

IIT Bombay

Abstract

Long range forecasts are the starting point of many decision support systems that need to draw inference from high-level aggregate patterns on forecasted values. State of the art time-series forecasting methods are either subject to concept drift on long-horizon forecasts, or fail to accurately predict coherent and accurate high-level aggregates.

In this work, we present a novel probabilistic forecasting method that produces forecasts that are coherent in terms of base level and predicted aggregate statistics. We achieve the coherency between predicted base-level and aggregate statistics using a novel inference method. Our inference method is based on KL-divergence and can be solved efficiently in closed form. We show that our method improves forecast performance across both base level and unseen aggregates post inference on real datasets ranging three diverse domains. Our code can be found at the following URL: <https://github.com/pratham16cse/AggForecaster>

1 Introduction

Long-term forecasting is critical for decision support in several application domains including finance, governance, and climate studies. Interactive decision making tools need accurate probability distributions not just over the long-term base forecasts but also on dynamically chosen aggregates of the forecasts. An analyst may be interested in a variety of aggregates such as average, sum, or trend of values within a window of granularity. For example, the base-level forecasts may be retail price of a commodity at a daily-level for the next two quarters, but the end user may also inspect average at weekly or monthly granularity, or change in price (inflation) from week to week. For the aggregates too, the user is interested in the associated uncertainty represented as a distribution that is coherent with the base distribution.

Classical forecasting methods [1, 2] fail on long-term forecasting because of the simplified parametric

assumptions. For example, ARIMA [1] assumes a linear relationship between *history* and *forecast horizon*. Recently, neural methods of forecasting [3] have gained much interest. Because of their expressive power, neural models can learn complex interactions between values in the history and forecast horizon of the time-series. Hence, neural models have been found to be more effective over classical methods on large time-series datasets with complex interactions [4–6].

A standard method for time-series forecasting using neural networks is the auto-regressive (AR) recurrent neural model [4, 7]. In AR models the output distribution captures the full joint dependency among all predicted values where the value at t depends on all values before it. During training we condition on true previous values but during inference we need to perform forward sampling where each predicted value is conditioned on sampled prior values. In long-term forecasting, such forward sampling suffers from drift caused by cascading errors [8]. A second major limitation of the AR model is that the joint distribution over the forecast variables is expressed via a black-box neural network. Marginalizing the distribution to obtain distribution over dynamically chosen aggregates will involve repeated sampling steps, which may incur huge latency during interactive analysis.

This has led to the emergence of non-auto-regressive (NAR) models which independently predict each variable in the forecast horizon conditioned on the history. NAR models have been shown to work better in practice both for medium-term and long-term forecasting [9–11]. Another major benefit of the NAR models is that during inference all values can be predicted in parallel, unlike in the AR method that entails sequential sampling. However, a limitation of the non-auto-regressive methods is that, in the raw form a time-series often contains noise that hinders a forecasting model from capturing top-level patterns in the series over long prediction horizons. In applications that involve analysis over aggregates of forecast values, these might give rise to non-smooth or

inconsistent aggregates.

In this paper we propose a novel method of preserving higher-level patterns in long-range forecasts of non-auto-regressive forecast models while allowing accurate and efficient computation of the distribution of dynamically chosen aggregates. Our key idea is to train the model to independently output various high-order statistics over the forecast values, along with the base-level forecasts. Aggregated values provide a noise-removed signal of how the series evolves in time. We use such signals to guide inference to capture top-level trends in the data. We formulate that as a task of obtaining a revised consensus distribution that minimizes the KL distance with each predicted aggregate and base forecasts. The consensus distribution is represented as a Gaussian distribution that can be easily marginalized. The parameters of the consensus can be obtained via an efficient numerical optimization problem.

Contributions

- We propose a probabilistic forecasting method that is more accurate than state of the art for long-term forecasting.
- Our method outputs an easy to marginalize joint distribution for computing accurate and coherent aggregate distributions over dynamically defined functions on forecast values.
- We propose an efficient inference algorithm for computing the consensus distribution.
- Empirical evaluation on benchmark datasets show that our method improves both base-level forecast accuracy, and accuracy of aggregates using both probabilistic metrics like CRPS and simple error metrics like mean absolute error (MAE).

2 Our Model

A time-series in our model is characterized by a sequence $(\mathbf{x}_1, y_1) \dots (\mathbf{x}_n, y_n)$ where $\mathbf{x}_t \in \mathbf{R}^d$ denotes a vector of input features and y_t is a real-value at a time t . We are given a prefix or history from such a series up to a present time T which we denote as H_T . Our goal is to predict future values $y_{T+1} \dots y_{T+R}$ given input features $\mathbf{x} = \mathbf{x}_{T+1} \dots \mathbf{x}_{T+R}$ and the history H_T . Unlike in conventional time-series forecasting where the interest is short-term (say R between 1 and 10), in long-term forecasting we focus on large values of R (say between 100 and 1000). We wish to capture the uncertainty of the prediction by outputting a distribution over the predicted values. We denote $\hat{P}(y_{T+1} \dots y_{T+R} | H_T, \mathbf{x})$ as the distribution output by the model for future time horizon given history H_T .

Our goal is not just to provide accurate probabilistic forecasts for the the base-level values but also for aggregates of these values. We cannot separately predict each aggregate of interest because these may not be coherent with each other or with the base-level forecasts. Also, the set of aggregate functions and granularity may be decided dynamically. Thus, we seek to explicitly marginalize a base-level distribution to get the distribution of aggregate quantities. Our goal is to ensure the computational ease of this step, since the exact form of the aggregate and the granularity window may be chosen dynamically during interactive analysis.

Our method seeks to retain the advantage of parallel training and inference that modern transformer-based NAR models offer. We train multiple NAR models for forecasting different types of aggregate functions at different levels of granularity. During inference we obtain a consensus distribution, as a joint Gaussian distribution that can be marginalized in closed form for computing distributions over linear aggregates defined dynamically during analysis. The consensus distribution is obtained by minimizing the KL distance with the various base and aggregate-level forecasts by an efficient inference algorithm. We present the details of each of these steps next.

2.1 Aggregate Functions We choose a set \mathcal{A} of aggregate functions depending on likely use in downstream analysis. This set does not need to include all possible aggregate functions to be used during analysis, since our method generalizes well to new aggregates even when trained with two aggregate functions. Each aggregate function A_i is characterized with a window size K_i and a fixed real vector $\mathbf{a}^i \in \mathbf{R}^{K_i}$ that denotes the weight of aggregated values. For each A_i , we create an aggregated series by aggregating on disjoint windows of size K_i in the original series. The j -th value in the i th aggregated series is the aggregation of the values $y_{(j-1)K_i+1} \dots y_{jK_i}$. We will use the notation $w_{i,j}$ to refer to the window of indices $[(j-1)K_i, \dots, jK_i]$ that the j -th value of the i th function aggregates. We denote i -th aggregate series as $z_1^i, \dots, z_{T_i}^i$ where $T_i = \frac{T}{K_i}$ and calculate as follows:

$$(2.1) \quad z_j^i = A_i(\mathbf{y}_{w_{i,j}}) = \sum_{r=1}^{K_i} a_r^i y_{r+(j-1)K_i}$$

In this work, we consider two aggregations – (i) average and (ii) trend. Average is just:

$$(2.2) \quad z_j^i = \sum_{r=1}^{K_i} \underbrace{\frac{1}{K_i}}_{a_r^i} y_{(j-1)K_i+r}$$

In trend aggregation, we compute slope of a linear fit on the values in each window as

$$(2.3) \quad z_j^i = \sum_{r=1}^{K_i} \underbrace{\left(\frac{r}{K_i} - \frac{K_i+1}{2K_i} \right)}_{a_r^i} \cdot y_{(j-1)K_i+r}$$

Trend aggregate of the window captures how the series evolves in time. A positive (negative) trend denotes that the value increases (decreases) as we move forward in the window. We show examples of a base-level time series and one computed aggregate (average) in Figure 1. Our framework can work with any aggregate like the above two that can be expressed as a linear weighted sum of its arguments.

For ease of notation we refer to the base-level also as an aggregate function A_0 with window size $K_i = 1$ and $\mathbf{a}^i = [1]$.

2.2 Forecast Method We train independent probabilistic forecasting models for the series corresponding to each aggregate $A_i \in \mathcal{A}$ which includes the original time-series as well. Our work is agnostic of the exact neural architecture used for the forecasts. We present details of the train these models in Section 2.3. During inference we use the known history H_T and the trained models to get forecasts $\hat{P}(z_j^i | H_T, \mathbf{x}_j)$ for each of the variables $z_1^i, \dots, z_{T_i}^i$ for each aggregate function A_i , which includes the base-level quantities.

Since models for all aggregates and for the original series are trained independently, these predicted distributions are not necessarily coherent. We infer a new consensus distribution $Q(y_{T+1} \dots y_{T+R})$ that minimizes the KL-distance with each of the forecast distributions. We choose a tractable form for Q : a multivariate Gaussian with mean $\boldsymbol{\mu} = [\mu_{T+1} \dots \mu_{T+R}]^T$ and covariance Σ . With this form we can compute the marginal distribution of aggregate variable z_j^i as:

$$(2.4) \quad Q_j^i = \mathcal{N}\left(\boldsymbol{\mu}_{w_{i,j}}^T \mathbf{a}^i, \mathbf{a}^{iT} \Sigma_{w_{i,j}} \mathbf{a}^i\right)$$

We use the notation $\Sigma_{w_{i,j}}$ to denote the sub-matrix of Σ that spans over the indices in $w_{i,j}$. Likewise for $\boldsymbol{\mu}_{w_{i,j}}$.

Using these we can write our objective of finding the parameters $\boldsymbol{\mu}$ and Σ so as to minimize the KL-distance with each forecast distribution as:

$$(2.5) \quad \min_{\boldsymbol{\mu}, \Sigma} \sum_{i \in \mathcal{A}} \sum_{j=T_i}^{T_i+R_i} D_{\text{KL}}\left(Q_j^i \parallel \hat{P}(z_j^i | \bullet)\right)$$

When the distribution of each forecast variable $\hat{P}(z_j^i | \bullet)$ is represented as a Gaussian with mean $\hat{\mu}(z_j^i)$

and variance $\hat{\sigma}(z_j^i)$, their KL distance can be expressed in closed form¹. Also, the optimization over the $\boldsymbol{\mu}$ and Σ terms separate out into two independent optimization problems. For $\boldsymbol{\mu}$ the objective is now:

$$(2.6) \quad \min_{\boldsymbol{\mu}} \sum_{i \in \mathcal{A}} \sum_{j=T_i}^{T_i+R_i} \frac{1}{\hat{\sigma}(z_j^i)^2} (\boldsymbol{\mu}_{w_{i,j}}^T \mathbf{a}^i - \hat{\mu}(z_j^i))^2$$

This is a convex quadratic objective that can be solved in closed form as

$$(2.7) \quad \boldsymbol{\mu}^* = \left[\sum_{i \in \mathcal{A}} \sum_{j=T_i}^{T_i+R_i} \frac{\tilde{\mathbf{a}}_j^i \tilde{\mathbf{a}}_j^{iT}}{\hat{\sigma}(z_j^i)^2} \right]^{-1} \left[\sum_{i \in \mathcal{A}} \sum_{j=T_i}^{T_i+R_i} \tilde{\mathbf{a}}_j^{iT} \hat{\mu} \right]$$

where we use $\tilde{\mathbf{a}}_j^i \in \mathbf{R}^R$ to denote the padded version of the indices $w_{i,j}$.

For Σ the objective is:

$$(2.8) \quad \min_{\Sigma} \sum_{i \in \mathcal{A}} \sum_{j=T_i}^{T_i+R_i} \frac{\mathbf{a}^{iT} \Sigma_{w_{i,j}} \mathbf{a}^i}{2\hat{\sigma}(z_j^i)^2} - \log(\mathbf{a}^{iT} \Sigma_{w_{i,j}} \mathbf{a}^i)$$

This objective cannot be solved in closed form but we follow a strategy to efficiently approximate it. We consider a simplification of Σ to be a low-rank matrix. Following [12] we express the covariance Σ in a tractable format as follows:

$$\hat{\Sigma} = \text{Diag}(\sigma^2) + VV^T$$

$$\hat{\Sigma} = \begin{pmatrix} \sigma_{T+1}^2 & \dots & 0 \\ & \ddots & \\ 0 & \dots & \sigma_{T+R}^2 \end{pmatrix} + \begin{pmatrix} v_{T+1} \\ \vdots \\ v_{T+R} \end{pmatrix} \begin{pmatrix} v_{T+1} \\ \vdots \\ v_{T+R} \end{pmatrix}^T$$

where $v_{T+r} \in \mathbf{R}^k$ is r -th row of V , and k is the chosen rank of the covariance matrix.

Using the above form of Σ , Equation 2.8 can be rewritten as:

$$(2.9) \quad \min_{V, \sigma} \sum_{i \in \mathcal{A}} \sum_{j=T_i}^{T_i+R_i} \frac{\tilde{\mathbf{a}}_j^{iT} [\text{Diag}(\sigma^2)] \tilde{\mathbf{a}}_j^i + (\tilde{\mathbf{a}}_j^{iT} V)^2}{2\hat{\sigma}(z_j^i)^2}$$

$$(2.10) \quad - \log(\tilde{\mathbf{a}}_j^{iT} [\text{Diag}(\sigma^2)] \tilde{\mathbf{a}}_j^i + (\tilde{\mathbf{a}}_j^{iT} V)^2)$$

With the above representation of the joint distribution $Q(y_T, \dots y_{T+R})$, the number of parameters needed to store the distribution is linear in R , and also we can compute the distribution of any linear aggregate efficiently.

¹ $D_{\text{KL}}(\mathcal{N}(\mu_q, \sigma_q^2) \parallel \mathcal{N}(\mu_p, \sigma_p^2)) = \frac{(\mu_q - \mu_p)^2 + \sigma_q^2}{2\sigma_p^2} - \log \frac{\sigma_q}{\sigma_p} - \frac{1}{2}$

ALGORITHM 2.1. 1: **Input:** Training data $\{(\mathbf{x}_1, y_1) \dots (\mathbf{x}_n, y_n)\}$, aggregate functions $\mathcal{A} = \{(\mathbf{a}_i, K_i)\}$, forecast horizon R .

- 2: **for** A_i in \mathcal{A} **do**
- 3: */*Train i -th aggregate model using training data for i -th aggregate */*
- 4: $\mathcal{D}_{\text{trn}}^i = z_1^i, \dots, z_{n/K_i}^i$.
- 5: $\theta^i \leftarrow \text{TRAIN}(\mathcal{D}_{\text{trn}}^i)$
- 6: $\hat{P}(z_j^i | \theta^i)$ denotes the forecasts for positions $j = T_i + 1, \dots, T_i + R_i$ in the forecast horizon.
- 7: **end for**
- 8: $\mathcal{K} = \{K_i | i = 1 \dots |\mathcal{A}|\}$.
- 9: Obtain coherent mean forecasts $\boldsymbol{\mu}^*$ using Eqn. 2.7.
- 10: Obtain coherent variance forecasts (V^*, σ^*) by solving Eqn. 2.9.
- 11: */* Compute new aggregate A_{new} on coherent forecasts */*
- 12: $\boldsymbol{\mu}^{*\text{new}} = \boldsymbol{\mu}^{*T} \tilde{\mathbf{a}}^{\text{new}}$.
- 13: $\Sigma^{*\text{new}} = (\tilde{\mathbf{a}}^{\text{new}})^T \Sigma^* (\tilde{\mathbf{a}}^{\text{new}})$.

2.3 Training As mentioned earlier we train separate models for each aggregate series. For each aggregate A_i the forecast model can be viewed function $F(H_T, \mathbf{x}_R | \theta^i)$ of the history of known values $H_T = (\mathbf{x}_1, y_1) \dots (\mathbf{x}_T, y_T)$, and known input features $\mathbf{x}_{T+1} \dots \mathbf{x}_{T+R}$ of the next R values for which the model needs to forecast. We use θ^i to denote the parameters of the i th forecast model. The exact form of the forecast model $F()$ that we used is described next, followed by a description of the training procedure.

2.3.1 Architecture of Forecast Model Our forecasting model $F(H_T, \mathbf{x}_R | \theta^i)$ is based on Transformers like the Informer model [11] but with subtle differences that provide gains even for the baseline predictions.

Our model first applies a convolution on the input \mathbf{z} series and input features \mathbf{x} . The Transformer’s multi-headed attention layers are on a concatenation of the convolution layer output.

$$\begin{aligned} \mathbf{z}^c &= \text{Conv}(\mathbf{z}, w_y, 1) & \mathbf{x}^c &= \text{Conv}(\mathbf{x}, w_f, 1) \\ \mathbf{h} &= \text{Transformer}([\text{Concat}(\mathbf{y}_t^c, \mathbf{x}_t^c) + \mathbf{e}_t : t = 1 \dots T]) \end{aligned}$$

where $\mathbf{h} \in \mathbb{R}^{T \times d_{\text{model}}}$ is the output of the transformer encoder and \mathbf{e}_t denotes the positional encoding of time index t . In the decoder, we *warm start* to provide more context to the decoder apart from the encoder state \mathbf{h} . In warm start, we select the last s values in the input

series and use them in the decoder of the transformer.

$$\begin{aligned} \mathbf{z}^c &= \text{CONV}([\mathbf{z}_{T-s+1 \dots T}, \mathbf{0}_R], w_z, 1) \\ \mathbf{x}^c &= \text{CONV}([\mathbf{x}_{T-s+1 \dots T}, \mathbf{x}_{T+1 \dots T+R}], w_x, 1) \\ \mathbf{h}_\mu &= \text{TransformerDecoder}_\mu(\text{Concat}(\mathbf{z}^c, \mathbf{x}^c) + \mathbf{e}, \mathbf{h}) \\ \mathbf{h}_\sigma &= \text{TransformerDecoder}_\sigma(\text{Concat}(\mathbf{z}^c, \mathbf{x}^c) + \mathbf{e}, \mathbf{h}) \\ \mu &= \text{Linear}(\mathbf{h}_\mu) & \sigma &= \text{Softplus}(\text{Linear}(\mathbf{h}_\sigma)) \end{aligned}$$

where $\mathbf{0}_R$ is a vector of zeros of length R , $\mathbf{h}_\mu \in \mathbb{R}^{R \times d_{\text{model}}}$, $\mathbf{h}_\sigma \in \mathbb{R}^{R \times d_{\text{model}}}$, $\mu \in \mathbb{R}^{R \times 1}$, and $\sigma \in \mathbb{R}^{R \times 1}$.

2.3.2 Training procedure We start with base level series $(\mathbf{x}_1, y_1) \dots (\mathbf{x}_n, y_n)$. First we split the series into training, validation, and test sets of lengths l_{trn} , l_{val} , and l_{test} respectively as follows:

$$\begin{aligned} \mathcal{D}_{\text{trn}} &= \{(\mathbf{x}_t, y_t) | t = 1, \dots, l_{\text{trn}}\} \\ \mathcal{D}_{\text{val}} &= \{(\mathbf{x}_t, y_t) | t = l_{\text{trn}} - T + 1, \dots, l_{\text{trn}} + l_{\text{val}}\} \\ \mathcal{D}_{\text{test}} &= \{(\mathbf{x}_t, y_t) | t = l_{\text{trn}} + l_{\text{val}} - T + 1, \dots, n\} \end{aligned}$$

Note that when $l_{\text{val}} \geq R$ or $l_{\text{test}} \geq R$, we use rolling-window setting as done in [10, 13] on validation and test sets.

We create training batches by sampling *chunks* of length $T + R$ from training set \mathcal{D}_{trn} as

$$\begin{aligned} \{(\mathbf{x}_t, y_t) | t = p, \dots, p + T + R\} \\ \text{where } p \sim [1, \dots, l_{\text{trn}} - (T + R - 1)] \end{aligned}$$

Similarly, we process i -th aggregate series $z_1^i, \dots, z_{n/K_i}^i$. Validation and test sets across base-level and aggregated series are aligned. To aggregate features, we simply take average value of each feature in the aggregation window for all aggregates. For an aggregate model for i -th aggregate with window size K_i , the forecast horizon is $R_i = \frac{R}{K_i}$. Similarly, the size of the history also changes. We set $T_i = B \frac{T}{K_i}$, so the aggregate model can effectively see the history B -times the size of base level model’s history. We found setting $B = 2$ works well in practice. It is also a good option for smaller datasets such as ETTH.

For each aggregate function A_i , we sample training chunks of size $T_i + R_i$ and train the parameters θ^i of the Transformer model for the following training objective.

$$(2.11) \quad \max_{\theta^i} \sum_{(\mathbf{x}_t^i, z_t^i)} \sum_{t=T_i+1}^{T_i+R_i} \log \mathcal{N}(z_t; (\mu_t, \sigma_t) = F(H_T, \mathbf{x}, t | \theta^i))$$

3 Related Work

Time series forecasting is an extensively researched problem. In deep learning, the problem got renewed interest [3] after an RNN-based auto-regressive model [4,

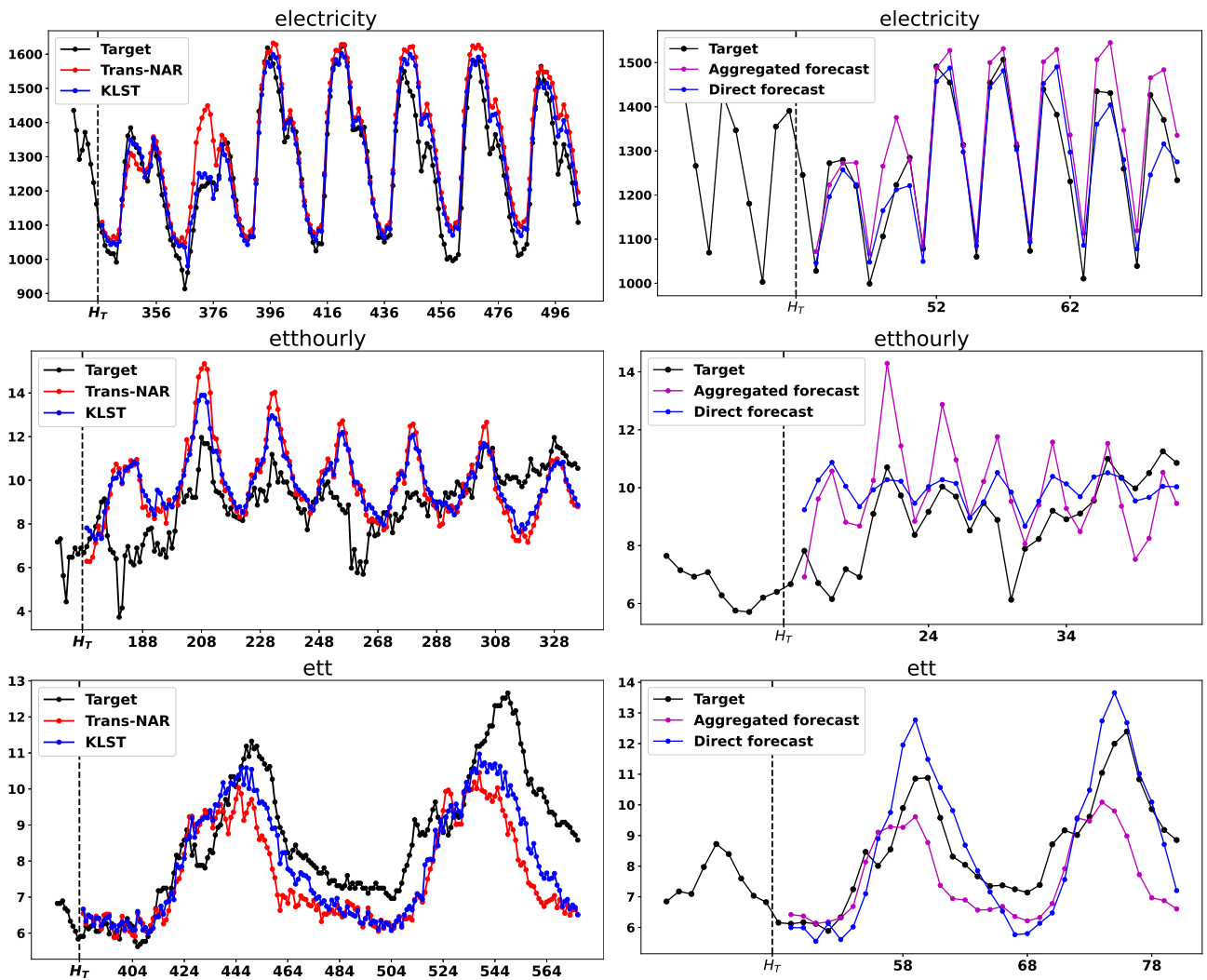


Figure 1: Left Column: Base level forecasts, Right Column: Forecasts of Sumaggregate with $K = 6$.

7] established conclusive gains over conventional machine learning and statistical methods. While these early neural models were based on RNNs, more recently Transformer-based models have been found to provide faster and efficient predictions on time-series data [5, 11, 14, 15]. For long-term forecasting autoregressive models are both slow and subject to cascading errors from previous predicted values for next-step predictions. Another option is non-auto-regressive models (NAR) which predict each future forecast independently in parallel [9–11]. However, since NAR models do not capture the joint distribution, they fail to provide accurate results for aggregate queries on forecasts. N-beats [6] is another recent architecture for time-series forecasting based on layered residual connections, specifically designed for interpretability. Our technique is orthogonal to the underlying time-series forecasting model.

Multi-level Models Our approach of independently predicting models at different aggregation levels and then reconciling is related to the approach in [17–19]. Their hierarchies are over items and consider only sum-based aggregates whereas we create hierarchies along time and consider arbitrary linear aggregates. Also, our objective is to minimize the KL distance with the distribution at various levels whereas they focus on error minimization and their parameterization of the reconciliation is different from ours. [20] is another multi-level model for item hierarchies that train models in a bottom up manner with higher level models regularized to be consistent with lower layers. They do not model inter-item correlation, can only efficiently handle fixed aggregates, and do not revise base-level forecasts. We obtain gains at the base-level too via the hierarchies that we create along the time dimension.

Beyond Base-level Forecasting Loss Our method of learning the slope as an aggregate in the forecast horizon is related to recent efforts at trying to learn the shape of the series. Recently, [21, 22] learn the shape of the series in forecast horizon using a differentiable approximation of Dynamic Time Warping (DTW) loss function. They also contain additional losses that minimize distortion and increase diversity. [23] capture moving statistics of the history through a recurrent layer. However, they use the statistics only to capture dependence among observed variables.

Long-term Forecasting Model Recently [11] proposed a Transformer architecture for long-range time-series forecasting. Their focus is to make the self-attention computation in transformer more efficient for long series by enforcing sparsity in the attention weights. To the best of our knowledge, this is the best performing current method for long-term forecasting. We compare

Dataset	Model	CRPS	MAE	MSE
ETT	Informer	7.01	7.01	61.67
	Trans-AR	2.56	3.76	19.83
	Trans-NAR	1.13	1.57	4.03
	KLST	1.10	1.52	3.75
Solar	Informer	41.01	41.015	2810
	Trans-AR	17.54	22.34	1683
	Trans-NAR	10.24	14.98	899
	KLST	10.21	14.99	886
ETTH	Informer	4.80	4.80	34.75
	Trans-AR	1.86	2.53	10.02
	Trans-NAR	1.55	2.22	7.45
	KLST	1.50	2.15	6.94
Electricity	Informer	172.3	172.3	44689
	Trans-AR	103.7	146.4	34702
	Trans-NAR	41.5	56.6	6475
	KLST	39.9	54.5	5972

Table 1: Comparison of KLST with three baseline models – (i) Informer, (ii) Trans-AR, and (iii) Trans-NAR using evaluation metrics CRPS, MAE, and MSE. On CRPS and MSE, KLST performs better than all the baselines whereas on MAE, KLST performs better than baselines in three out of four cases.

empirically with this model and present significant gains on multiple datasets.

4 Experiments

We evaluate our method on four real-life datasets and contrast with state-of-the-art methods of long-term forecasting.

4.1 Datasets

Electricity [24] This dataset contains national electricity load at Panama power system. The dataset is collected at an hourly granularity and over the span of five years from January 2015 to June 2020. However, in this work we use the data up to March 2020 to create training, validation and test sets.

Solar This dataset comprises of hourly photovoltaic production of 137 stations in Alabama state and has been used in [12].

ETT (Hourly and 15-minute) [25] The Electricity Transformer Temperature (ETT) datasets contains a time-series of oil-temperature at an electrical transformer. The dataset is available at two granularities, one with 15 minute interval (ETT) and another with one hour interval (ETTH). The entire dataset is collected over the span of two years, from July 2016 to June 2017. Both the variants are used in [11].

4.2 Base Models

Informer [11] is a recent Transformer based model specifically designed for long-term forecasting. They also use a non-auto-regressive model and predict each future value independently.

Trans-NAR refers to our Transformer architecture described in Section 2.3.1 but where we predict only a single model on only the base-level forecasts.

Trans-AR Trans-AR is an autoregressive version of the transformer architecture described in Section 2.3.1. Trans-AR sequentially predicts values in the forecast horizon. At the t -th step during prediction, it performs convolution on the window $\hat{z}_{t-w_y+1}, \dots, \hat{z}_{t-1}$ of predicted values. Whenever $t < w_f$, the convolution window overlaps with the history H_T . In such cases, the transformer uses observed values from H_T for convolution.

KLST refers to our method where we independently train a base level model and aggregate models as described in Section 2.3. We then apply the inference procedure described in Section 2.2 to obtain the coherent forecasts. Here we use Sumand Slopeaggregates of the base level data to train the aggregate models. The set of K values that we use are as follows: For Electricity and Solar, we use $K = \{2, 6, 12\}$. For ETT, we have used $K = \{4, 6, 12\}$ and for ETTH we use $K = \{2, 6\}$. We fixed these K values by visually analyzing the data and by selecting the K values that could potentially better represent the top-level trends in the dataset.

4.3 Evaluation Metrics In order to evaluate probabilistic forecasts, we use Continuous Ranked Probability Score (CRPS) metric. CRPS is a proper scoring rule [26] and widely used for evaluating probabilistic forecasts [12]. If we denote the predicted CDF for a target value y_t by $F_t(\cdot)$, we can write the CRPS by integrating the quantile loss over all possible quantiles [12]:

$$(4.12) \quad \Lambda_\alpha(q, y_t) = (\alpha - \mathcal{I}_{[y_t < q]})(y_t - q)$$

$$(4.13) \quad \text{CRPS}(F_t^{-1}, y) = \int_0^1 2\Lambda_\alpha(F^{-1}(\alpha), y_t) d\alpha$$

We also evaluate the point forecasts, which are essentially means of the predictive distributions, using Mean Absolute Error (MAE) and Mean Squared Error (MSE).

Dataset	# Series	Avg. T	R	train-len. /series	test-len. /series
ETT	1	384	192	55776	13824
ETTH	1	168	168	14040	3360
Electricity	1	336	168	36624	9072
Solar	137	336	168	7009	168

Table 2: Summary of the datasets

Dataset	Model	K	CRPS
ETT	Trans-NAR	1	1.133
	KLST	4,6,12	1.099
		4	1.103
		6	1.117
		12	1.122
Solar	Trans-NAR	1	10.242
	KLST	2,6,12	10.208
		2	10.332
		6	10.225
		12	10.094
ETTH	Trans-NAR	1	1.547
	KLST	2,6	1.498
		2	1.502
		6	1.524
Electricity	Trans-NAR	1	41.527
	KLST	2,6,12	39.937
		2	40.356
		6	40.792
		12	40.738

Table 3: Effect of performing inference using single K value versus multiple K values. In all datasets except Solar, using multiple K values yields better forecasts than using single K value.

4.4 Results

4.5 Qualitative results We present some anecdotes to provide insights on why KLST should enhance the accuracy of base-level forecasts. In Figure 1 (left column) we show that forecasts by KLST (blue) are closer to the ground truth (black) compared to the base-level model Trans-NAR (red). We explain this is due to the improved accuracy of the model that independently predicts the sum aggregate for a window of $K = 6$. In the right column of Figure 1 we show the forecast by aggregating the base-level forecasts from Trans-NAR, and the direct forecast from a model specifically trained for the aggregate. We observe that direct forecast values are much closer to the ground-truth than those from aggregating base-level forecasts. When these improved aggregates are used to revise the base-level forecasts to be consistent with these aggregates (as described in Section 2.2), we obtain better forecasts at the base-level.

4.6 Impact of KLST on Long-Term Forecasts

In Table 3, we compare KLST with Informer, Trans-NAR, and Trans-AR (described in Sec. 4.2). The comparison shows that KLST performs better than all baselines in terms of CRPS, and MSE. For MAE, KLST performs better than baselines on three out of four datasets,

and is almost the same on the fourth. In comparison to Trans-NAR, we observe small or no improvement on Solar dataset primarily because of the predictive nature of this dataset. The y value in Solar is strongly dependent on the hour-of-day feature. Any other factor(s) that affect the y value are external and cannot be modelled with the available data. The Electricity dataset also follows a pattern that is heavily dependent on hour-of-day. However, energy consumption also depends of day-of-week. Hence, for long-range forecasting, the aggregate models can better capture top level trends in the data that the base level model might find difficult (first row in Fig. 1). This results in better performance of KLST on Electricity dataset.

4.7 Results on Unseen Aggregates Post Inference An important aspect of time-series analytics is the effectiveness of base-level forecasts on various types of aggregates at various granularities. Training an aggregate model for each aggregate and at each granularity is rather expensive. Our approach is to train a few representative aggregate models using a fixed set of K_i values. Then, forecasts after consensus can be used to compute other aggregate and at other granularities.

In Figure 2, we compare KLST with Trans-NAR using three aggregates and seven K values. The set of K values we use in Fig. 2 also contain the K for which no aggregate model is trained. Also, no aggregate model was trained corresponding to the Diff aggregate. For each aggregate and for each K , first we aggregate the Trans-NAR forecasts and KLST forecasts. Then we plot the reduction in the CRPS values of KLST over Trans-NAR. We see that in most cases reduction is positive, indicating that CRPS of Trans-NAR is higher than KLST. For Solar we observed no difference because of reasons mentioned earlier, and is therefore skipped from these graphs. However, for some of the other datasets, specifically Electricity, the gains are significant.

4.8 Effect of training with Single- K vs multiple- K values In Table 3, we compare the effect of using single K values versus multiple K values in KLST. On three of four datasets, we observe that using all K values instead of using a single K is the most effective approach.

5 Conclusion

In this paper we addressed the problem of long-range forecasting with the goal of providing accurate probabilistic predictions, not just at the base-level but also at dynamically chosen aggregates. We proposed a simple method of independently training forecast models at different aggregation levels, and then designing a con-

sensus distribution to minimize distance with forecasts from each component distribution. We obtained significant gains in accuracy over the base-level and over new aggregate functions at new granularity levels defined during test time. Future work include extending our method to fit quantiles instead of mean and variance.

References

- [1] G. Box and G. M. Jenkins, "Some recent advances in forecasting and control," *Journal of Royal Statistical Society. Series C (Applied Statistics)*, vol. 17, no. 2, pp. 91–109, 1968.
- [2] R. Hyndman, A. Koehler, J. Ord, and R. Snyder, *Forecasting with exponential smoothing: The state space approach*. Springer, 2008.
- [3] K. Benidis, S. S. Rangapuram, V. Flunkert, B. Wang, D. Maddix, C. Turkmen, J. Gasthaus, M. Bohlke-Schneider, D. Salinas, L. Stella *et al.*, "Neural forecasting: Introduction and literature overview," *arXiv preprint arXiv:2004.10240*, 2020.
- [4] V. Flunkert, D. Salinas, and J. Gasthaus, "Deepar: Probabilistic forecasting with autoregressive recurrent networks," *CoRR*, vol. abs/1704.04110, 2017.
- [5] S. Li, X. Jin, Y. Xuan, X. Zhou, W. Chen, Y.-X. Wang, and X. Yan, "Enhancing the locality and breaking the memory bottleneck of transformer on time series forecasting," in *Advances in Neural Information Processing Systems*, 2019, pp. 5243–5253.
- [6] B. N. Oreshkin, D. Carpov, N. Chapados, and Y. Bengio, "N-beats: Neural basis expansion analysis for interpretable time series forecasting," *arXiv preprint arXiv:1905.10437*, 2019.
- [7] S. Mukherjee, D. Shankar, A. Ghosh, N. Tathawadekar, P. Kompalli, S. Sarawagi, and K. Chaudhury, "ARMDN: associative and recurrent mixture density networks for etail demand forecasting," *CoRR*, vol. abs/1803.03800, 2018.
- [8] P. Deshpande, K. Marathe, A. De, and S. Sarawagi, "Long horizon forecasting with temporal point processes," in *ACM WSDM*, 2021. [Online]. Available: <https://doi.org/10.1145/3437963.3441740>
- [9] R. Wen, K. Torkkola, and B. Narayanaswamy, "A multi-horizon quantile recurrent forecaster," *arXiv preprint arXiv:1711.11053*, 2017.
- [10] P. Deshpande and S. Sarawagi, "Streaming adaptation of deep forecasting models using adaptive recurrent units," in *ACM SIGKDD*, 2019.
- [11] H. Zhou, S. Zhang, J. Peng, S. Zhang, J. Li, H. Xiong, and W. Zhang, "Informer: Beyond efficient transformer for long sequence time-series forecasting," *arXiv preprint arXiv:2012.07436*, 2020.
- [12] D. Salinas, M. Bohlke-Schneider, L. Callot, R. Medico, and J. Gasthaus, "High-dimensional multivariate forecasting with low-rank gaussian copula processes," in

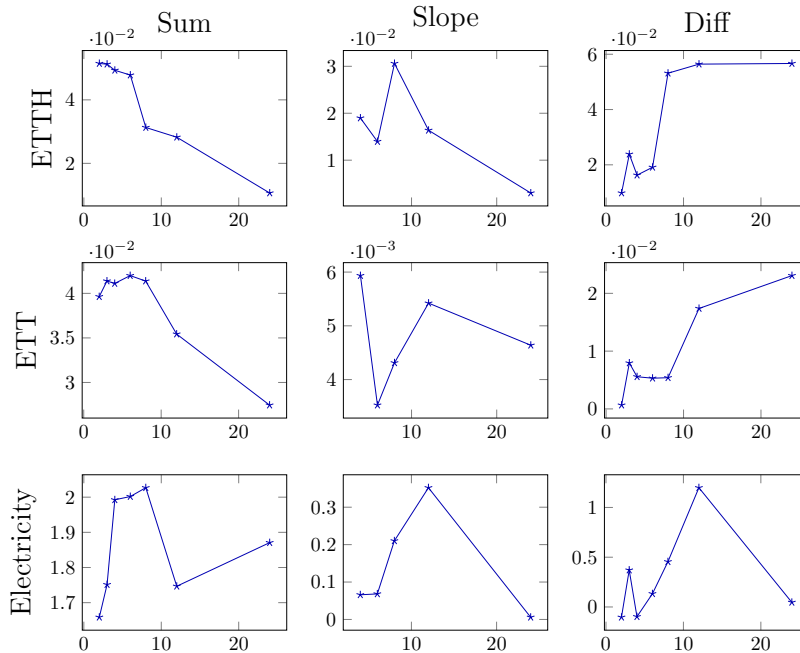


Figure 2: Reduction in CRPS of KLST over the baseline Trans-NAR model on three datasets (along rows) and three aggregates (along columns). X-axis is the window size of aggregation.

- Advances in Neural Information Processing Systems*, 2019, pp. 6827–6837.
- [13] S. S. Rangapuram, M. W. Seeger, J. Gasthaus, L. Stella, Y. Wang, and T. Januschowski, “Deep state space models for time series forecasting,” in *Advances in Neural Information Processing Systems 31*, S. Bengio, H. Wallach, H. Larochelle, K. Grauman, N. Cesa-Bianchi, and R. Garnett, Eds., 2018, pp. 7796–7805.
- [14] B. Lim, S. O. Arik, N. Loeff, and T. Pfister, “Temporal fusion transformers for interpretable multi-horizon time series forecasting,” 2020.
- [15] P. Bansal, P. Deshpande, and S. Sarawagi, “Missing value imputation on multidimensional time series,” *arXiv preprint arXiv:2103.01600*, 2021.
- [16] J. Gasthaus, K. Benidis, Y. Wang, S. S. Rangapuram, D. Salinas, V. Flunkert, and T. Januschowski, “Probabilistic forecasting with spline quantile function rnns,” in *The 22nd International Conference on Artificial Intelligence and Statistics*, 2019, pp. 1901–1910.
- [17] S. B. Taieb, J. W. Taylor, and R. J. Hyndman, “Coherent probabilistic forecasts for hierarchical time series,” in *International Conference on Machine Learning*, 2017, pp. 3348–3357.
- [18] S. Ben Taieb and B. Koo, “Regularized regression for hierarchical forecasting without unbiasedness conditions,” in *Proceedings of the 25th ACM SIGKDD International Conference on Knowledge Discovery and Data Mining*, 2019.
- [19] S. L. Wickramasuriya, G. Athanasopoulos, and R. J. Hyndman, “Optimal forecast reconciliation for hierarchical and grouped time series through trace minimization,” *Journal of the American Statistical Association*, vol. 114, no. 526, pp. 804–819, 2019.
- [20] X. Han, S. Dasgupta, and J. Ghosh, “Simultaneously reconciled quantile forecasting of hierarchically related time series,” in *Proceedings of The 24th International Conference on Artificial Intelligence and Statistics*, 2021, pp. 190–198.
- [21] V. LE GUEN and N. THOME, “Shape and time distortion loss for training deep time series forecasting models,” in *Advances in Neural Information Processing Systems 32*, 2019.
- [22] V. L. Guen and N. Thome, “Probabilistic time series forecasting with structured shape and temporal diversity,” *arXiv preprint arXiv:2010.07349*, 2020.
- [23] J. B. Oliva, B. Póczos, and J. G. Schneider, “The statistical recurrent unit,” in *ICML*, 2017, pp. 2671–2680.
- [24] “Electricity load forecasting panama.” [Online]. Available: <https://data.mendeley.com/datasets/byx7sztj59/1>
- [25] “Electricity transformer temperature.” [Online]. Available: <https://github.com/zhouhaoyi/ETDataset>
- [26] T. Gneiting and A. E. Raftery, “Strictly proper scoring rules, prediction, and estimation,” *Journal of the American statistical Association*, vol. 102, no. 477, pp. 359–378, 2007.